Iranian Journal of Basic Medical Sciences

ijbms.mums.ac.ir

IJBMS

The effect of platelet-rich plasma on human mesenchymal stem cell-induced bone regeneration of canine alveolar defects with calcium phosphate-based scaffolds

Reihaneh Shafieian [1], Maryam Moghaddam Matin [2], Amin Rahpeyma [3], Alireza Fazel [4, 5], Hamideh Salari Sedigh [6], Ariane Sadr-Nabavi [7], Halimeh Hassanzadeh [2], Alireza Ebrahimzadeh-Bideskan [4, 5*]

[1] Department of Anatomy and Cell Biology, School of Medicine, Mashhad University of Medical Sciences, Mashhad, Iran
[2] Stem Cell and Regenerative Medicine Research Group, Academic Center for Education, Culture, and Research (ACECR), Khorasan Razavi Branch, Mashhad, Iran
[3] Oral and Maxillofacial Diseases Research Center, School of Dentistry, Mashhad University of Medical Sciences, Mashhad, Iran
[4] Microanatomy Research Center, School of Medicine, Mashhad University of Medical Sciences, Mashhad, Iran
[5] Department of Anatomy and Cell Biology, School of Medicine, Mashhad University of Medical Sciences, Mashhad, Iran
[6] Department of Clinical Sciences, Faculty of Veterinary Medicine, Ferdowsi University of Mashhad, Mashhad, Iran
[7] Department of Genetics, School of Medicine, Mashhad University of Medical Sciences, Mashhad, Iran

ARTICLE INFO

Article type:
Original article

Article history:
Received: Mar 5, 2017
Accepted: Aug 10, 2017

Keywords:
Adipose tissue
Bone
Dog
Osteogenesis
Stem cells
Tissue engineering

ABSTRACT

Objective(s): Autologous bone transplantation known as the "gold standard" to reconstruction of osseous defects has known disadvantages. This study was designed to explore the effects of hydroxy-apatite/tricalcium-phosphate (HA/TCP) and platelet-rich plasma (PRP) on the osteogenesis ability of human adipose-derived mesenchymal stem cells (hAdMSCs) *in vitro* and *in vivo*.

Materials and Methods: hAdMSCs were incubated with HA/TCP granules and/or PRP *in vitro* and then, cell proliferation and differentiation was assessed by MTT assay, AZR S staining and SEM examination. *In vivo*, four cylindrical defects were drilled in the mandibular bones of 5 mongrel dogs and divided randomly into the following groups: I-autologous crushed bone, II- no filling material, III- HA/TCP and PRP, IV- PRP-enriched hAdMSCs seeded on HA/TCP granules. Inserted hAdMSCs were labeled to trace their contribution to bone tissue regeneration. Finally, cell tracing and tissue regeneration were evaluated by immunohistochemistry and histomorphometry methods, respectively.

Results: *In vitro*, co-incubation with HA/TCP granules significantly reduced proliferation and osteogenic differentiation ability of hAdMSCs; while PRP application promoted these capacities (P<0.05). *In vivo*, PRP-enriched hAdMSCs seeded on HA/TCP granules induced considerable bone formation in osseous defects (P<0.05). It was obviously shown that hAdMSCs were incorporated into the newly-formed bone.

Conclusion: Based on this study, application of stem cells could offer a helpful therapeutic tool in bone tissue regeneration. Although inserted hAdMSCs were identifiable throughout the newly-formed bone tissue, their few number could be an indicator of indirect role of hAdMSCs in tissue regeneration.

► *Please cite this article as:*
Shafieian R, Moghaddam Matin M, Rahpeyma A, Fazel AR, Salari Sedigh H, Sadr-Nabavi A, Hassanzadeh H, Ebrahimzadeh-Bideskan AR. The effect of platelet-rich plasma on human mesenchymal stem cell-induced bone regeneration of canine alveolar defects with calcium phosphate-based scaffolds. Iran J Basic Med Sci 2017; 20:1131-1140. doi: 10.22038/IJBMS.2017.9447

Introduction

Due to the formerly-declared disadvantages of autologous bone transplantation known as the "gold standard" approach to reconstruction of osseous defects, bone tissue engineering (BTE) strategies have gathered raised interest to accomplish this goal, especially in the craniofacial skeleton (1). Stem cell delivery via application of scaffolds alone or enriched by different growth factors have been widely documented to be a reliable approach in regenerative medicine (2). Among various well-known mesenchymal stem cell sources, adipose-derived mesenchymal stem cells (AdMSCs) have been evaluated to present superior advantages over other sources of mesenchymal stem cells including high availability and insignificant donor site morbidity during their provision, which make them a suitable alternative in tissue engineering procedures (3, 4). Scaffolds act as a delivery system for transferring stem cells to the desired damaged site (2). Alongside with good mechanical properties, a suitable scaffold in BTE should display high degrees of biocompatibility and osteoconductivity in order to mimic the natural microenvironment of bone tissue (5). Porous hydroxyl-apatite/tricalcium-phosphate (HA/TCP) ceramics are one of the most accepted synthetic graft biomaterials used clinically for bone tissue engineering due to their excellent biocompatibility and re-absorbability (6, 7). Indeed, calcium-phosphate-based scaffolds present a

*Corresponding author: Alireza Ebrahimzadeh-Bideskan. Department of Anatomy and Cell Biology, School of Medicine, Mashhad University of Medical Sciences, Mashhad, Iran. Tel: +98-513-8002486; Fax: +98-513-8002487; email: EbrahimzadehBA@mums.ac.ir

similar composition and structure to the mineralized bone tissue and thus, are expected to expedite and promote cell attachment and signaling, which are among essential characteristics demonstrated for a suitable scaffold (2).

HA/TCP ceramics are known to be a rich source of calcium and phosphorus, which are highly needed during the process of bone deposition and remodeling (8).

Furthermore, enhanced bone tissue regeneration can be expected by addition of appropriate growth factors to the calcium-phosphate-based scaffolds (5).

Growth factors are biologically active agents present in different tissues and organs that mediate important signal transferring between cells and their microenvironment and subsequently provide an osteoinductive property in tissue regeneration field (9). Platelet-rich plasma (PRP) is a super-mixture of imperative growth factors contained in platelets' granules which upon their release, govern a cascade of neovasculogenesis and tissue repair procedures, leading to introduce PRP as a therapeutic implementation in bone regeneration (10, 11).

Taken as a whole, this study aimed to explore the effect of pre-synthesized porous HA/TCP granules and PRP on the osteogenesis ability of human adipose-derived mesenchymal stem cells (hAdMSCs) *in vitro* and *in vivo*. In our study, inserted hAdMSCs *in vivo* were labeled and tracked to obtain more evidence on their biodistribution and possible contribution to bone tissue regeneration.

To the best of our knowledge, this is the first study conducted to investigate the *in vivo* fate and probable regenerative involvement of transplanted mesenchymal stem cells (MSCs) into canine large-sized osseous defects. This could be helpful to future speculation of stem cell therapy in clinical chair side approaches.

Materials and Methods

Preparation of MSCs, PRP, and biomaterial

hAdMSCs isolation and expansion

Use of human MSCs was approved by Ethical Committee Acts of Mashhad University of Medical Sciences (Ethical approval number: 940024). AdMSCs were isolated and expanded as reported earlier (4). Briefly, liposuction aspirates of subcutaneous adipose tissue were obtained from healthy individuals volunteered for routine plastic surgery at a medical center. After extensive washing with phosphate-buffered saline (PBS) complemented with antibiotics (100 U/ml of penicillin and 100 µg/ml of streptomycin) (PS) (Invitrogen), the samples were incubated for 60 min with 0.1% collagenase type I (Invitrogen) in PBS at 37 °C, receiving short, robust agitations every 15 min. Collagenase digestive activity was neutralized with 10% fetal bovine serum (FBS) (Gibco) followed by centrifugation at 800 g for 5 min. After removing the supernatant, the remaining pellet was resuspended and cultured in T75 flasks (Nunc) and Dulbecco's modified Eagle's medium with low glucose (DMEM-LG) supplemented with 10% FBS and 1% PS was added to the culture plates afterwards. After a 72 hr period of incubation at 37 °C with 5% CO_2, cultured cells were washed with PBS to remove the unattached cells and nourished with fresh medium. The medium was replaced every two days and upon reaching 70-80% confluency, cells were detached and re-plated into new flasks at a density of 5000–10000 cells/cm^2. Intermittent passages were repeated till passage 3 (P3) from which cells were trypsinized (0.025%; Invitrogen) and subjected to flowcytometric analysis (FACScalibur, BD Bioscience) to verify the expression of specific cell surface antigens. Our employed antibodies for fluorescence-activated cell sorting (FACS) study included mouse anti-CD44 polyclonal antibody, rabbit anti-CD34 polyclonal antibody (Antibodies-online, Germany), mouse anti-CD90 monoclonal antibody, rabbit anti-CD11b polyclonal antibody (Novus Biologicals, USA), rabbit anti-CD105 polyclonal antibody, and rabbit anti-CD45 polyclonal antibody (Bioss Inc., USA) (12).

In vitro differentiation assay

To confirm the identity of isolated AdMSCs, *in vitro* differentiation of P3 cells towards osteogenic and adipogenic lineages was assayed (4). The fibroblastic mesoderm-derived phenotype of isolated cells was induced via maintenance in standard growth medium; while osteogenic differentiation was encouraged via replenishment by osteogenic induction medium composed of DMEM with 10% FBS, 50 µg/ml ascorbate-2-phosphate, 100 nM dexamethasone and 10 mM β-glycerol phosphate (Sigma) for a period of 21 days. Upon the end of this time, cells were fixed in ethanol and incubated with 0.1% Alizarin Red (AZR) S (Sigma) to stain the deposited minerals. Lengthwise, adipogenic differentiation was prompted via treatment with 50 mg/ml ascorbate-2-phosphate, 100 nM dexamethasone and 50 mg/ml indomethacin (Sigma) for up to 3 weeks. Finally, the cells were fixed with 10% formalin and incubated with 0.5% Oil red O (Sigma) to stain the intracellular fat vacuoles. All experiments were performed in triplicate to validate statistical analyses.

HA/TCP biomaterial provision

Synthetic graft biomaterials composed of HA/TCP granules with the ratio of 30:70 (%weight) (OSTEON™ II, Korea) were chosen for this study due to high similarity to natural bone mineral composition (13). Manipulated biphasic calcium-phosphate (BCP) granules consumed in this study ranged within 0.5-2 mm in size with the general porosity of estimated 70±5 (%volume). This biomaterial was provided in double-sealed packaging and sterilized by gamma-irradiation.

HA/TCP Scaffold/ hAdMSCs construcs

P3 hAdMSCs destined to be inserted into osseous defects were incubated with 5 μM BrdU (5-bromo-2′deoxy-uridine) (Sigma) for 48 hr before transplantation. BrdU is a synthetic analog of thymidine, gets integrated into the newly-forming DNA strands during S phase of cell division and thus, is considered as a kind of nuclear gene-transfer free dye with high efficacy in enduring cell tracking means (14).

Finally, hAdMSCs with a concentration of 1×10^6 cells diluted in 2 ml medium, were seeded drop-wise onto HA/TCP granules and allowed to attach to the prepared scaffold for 24 hr prior to implantation into the osseous defects.

Scanning electron microscopy (SEM) assessment

Qualitative analysis of HA/TCP granules sub-cultured with hAdMSCs was conducted through SEM observation (Leo, Germany) (15). Firstly, prepared scaffold/hAdMSCs constructs were fixed with 2.5% glutaraldehyde for 60 min. Following extreme rinsing with PBS and dehydration through ascending concentrations of ethanol, the specimens were dried thoroughly, sputter-coated with gold and went under SEM. SEM observation of a non-cultured scaffold served as control.

Preparation of PRP

PRP was prepared based on differential centrifugation as described elsewhere (3, 16). Fifteen ml of venous blood was drawn from the jugular vein of each animal into sterile tubes containing citrate-phosphate-dextrose as an anticoagulant factor and underwent a two-step centrifugation method, including a first 10 min centrifugation step at 250 g in order to separate red blood cells from the blood. Subsequently, the supernatant plasma and buffy coat were pipetted, transferred to another tube and was subjected to another round of centrifugation at 1000 g for 10 min at room temperature. Successively, two phases were obtained including PRP at the bottom and PPP (platelet-poor plasma) at the upper portion of the tube. After buffering the PRP phase to the physiologic level, it was activated via intermittent cycles of freeze and thaw for further application.

In vitro evaluation of the effects of PRP and HA/TCP granules on hAdMSCs

Cell proliferation assay

To investigate the effects of pre-synthesized HA/TCP ceramics and PRP on cell proliferation capacity of hAdMSCs, cells were seeded on 24-well plates at a density of 5×10^4 cells/well, according to the following groups: 1-MT group: hAdMSCs + HA/TCP granules (30 μg/ml), 2-MP group: hAdMSCs + PRP 20% (by volume) and 3-MTP group: hAdMSCs + HA/TCP granules (30 μg/ml) + PRP 20%. HA/TCP granules without seeded cells were considered for normalization (control group). 3, 5 and 11 days following the treatments, all groups were incubated with 5 mg/ml MTT (3-(4, 5-dimethylthiazol-2-yl)-2, 5-dimethyl tetrazolium bromide) (Sigma) for 4 hr, followed by addition of 1 ml dimethyl sulfoxide (DMSO) to allow the produced intracellular formazan become visualized. Absorbance was quantified at 570 nm using a microplate reader (Bio-Rad, CA). Results were normalized with the control group consisted of just HA/TCP granules. All experiments were performed in triplicate to validate statistical analyses.

Mineralized nodule formation

Formation of mineralized nodules in experimental and control groups was investigated via AZR S staining after 14 and 21 days of incubation in the osteogenic induction medium (3). 1% AZR S staining buffer solution was prepared by adding 1 g AZR to 1% Tris-HCl solution. After washing with PBS and fixation with 95% ethanol, 10% cetylpyridinium chloride in Na_2HPO_4 was added to cells and the absorbance was then quantified at 562 nm using a microplate reader (Bio-Rad, CA). All the experiments were performed in triplicate to validate statistical analyses.

In vivo evaluation of PRP and HA/TCP granules with and without hAdMSCs

Animals and surgical procedures

The animal experiments conducted in this study were in accord with the ethical committee acts of the Ethical Committee for Animal Care and Use of Mashhad University of Medical Sciences, Ethical Committee Acts (approval number:940024). All animal procedures were performed in accordance with National Institutes of Health (NIH) and Animal Research Reporting of *In Vivo* Experiments (ARRIVE) animal care guidelines. Five adult male mongrel dogs with the mean age of 2 years were selected for this study. Upon arrival, animals were verified to be healthy through clinical examination and hematologic analysis. After health confirmation, each of them was weighed, vaccinated and housed at an individual cage at Animal Research Center of Dentistry Faculty of Mashhad University of Medical Sciences, provided with controlled temperature (20±2 °C), lighting (12 hr; light: 12 hr; dark photoperiod), and *ad libitum* access to water and commercially balanced dry food (France). After two weeks of adaption, all mandibular premolars at both sides were extracted carefully under general anesthesia and a four-week period was given to the soft tissue for spontaneous healing and repair. Prior to any surgical procedures, each animal was premeditated by an IM injection of 2 mg/kg xylazine-HCl (Alfasan, Netherlands). General anesthesia was induced via IV injection of 10 mg/kg ketamin-HCl (Alfasan, Netherlands) and 0.5 mg/kg diazepam (ZEPADICVR, Iran). General anesthesia was maintained under the supervision of a veterinarian

(SS.H.). All surgical procedures were performed under aseptic conditions. Edentulous sites were exposed by mucoperiosteal flaps and under constant irrigation, two cylindrical through-and-through defects in each side, perpendicular to the lateral cortex, were drilled using a 10-mm diameter trephine bur. Then, surgically-created defects were treated randomly as follows: I: autologous crushed mandibular bone (positive control), II: no filling material (negative control), III: HA/TCP granules in combination with PRP, and IV: PRP-enriched hAdMSCs seeded on HA/TCP granules. At last, the flaps were closed using restorable sutures and for the next 3 days, all operated animals received IM analgesic (2 mg/kg tramadol) and antibiotic (22 mg/kg ceftriaxone) medication. During the next week after surgery, the animals were examined daily for any sign of intraoral infection or wound dehiscence which were the exclusion criteria from the study.

Histological examination

Eight weeks after surgery, all animals were sacrificed by an IV overdose injection of sodium pentobarbital under general anesthesia. Mandible of each dog was cut away from the anterior border of the ramus and after a macroscopic examination, the center of implanted sites underwent sample retrieval using a 2-mm diameter trephine bur. Overall, a total of 20 thorough-and-thorough mandibular defects of 5 mongrel dogs divided into 4 experimental groups (n=5) went under sample retrieval for further examination; while 5 more samples, considered as the normal control group, were obtained from the buccal side of mandibular alveolar bone of every individual animal (a total of 25 samples for further examination). After fixation and decalcification, tissue samples were stained with AZR S and investigated using an optical microscope (17).

Histomorphometrical analysis

AZR S-stained sections, from a total of 25 samples divided in 5 groups, were evaluated for morpho metrical measurement of newly-formed bone surface area under 20x magnification of an optical microscope (BX51, Olympus, Japan) equipped with a digital camera (Canon, IXUS 950 IS) which was connected to a computer for using image software. Consecutive images from 5 randomly-chosen slides were analyzed for morphometrical measurement of the new-engineered bone surface area, quantified according to the previously-described formula (13).

In vivo cell tracing

Tissue sections were immunohistochemically stained to determine the biodistribution of implanted BrdU-labeled stem cells of human origin. Furthermore, extracellular matrix production by the inserted cells was verified through immunohistochemistry staining of human osteocalcin protein. To do this, primary rabbit antibodies against BrdU (Santa Cruz Biotechnology, Inc.) and human osteocalcin (ab93876, Abcam, USA) were used as described earlier (18). Briefly, following deparaffinization with xylene and rehydration through descending concentrations of ethanol, tissue sections were washed with antigen retrieval solution composed of citrate buffer 0.01 M (S2031, Dako, England) for 15 min. Endogenous peroxidase activity was obstructed through careful bathe in 3% H_2O_2 in methanol in the dark for 20 min. Subsequently, sections were washed thoroughly in PBS plus 0.025% Triton X-100 for three times, followed by 60 min of gentle rinse with 10% normal goat serum (ab7481, Abcam, USA) for non-specific antigen blockage. Ultimately, all the treated sections were soaked in primary antibody (diluted 20 to 1000 in PBS with 1% BSA) and stored overnight at 4 °C. The day after, all the sections were extremely washed with PBS and then incubated with HRP-conjugated secondary antibody (goat anti-rabbit IgG, ab6721, Abcam, USA) for 60 min at room temperature. Following extensive washing with PBS, all sections were treated with diaminobenzidine (DAB) solution (DAB kit, Sigma Aldrich, USA) to make the fabricated antigen-antibody complexes visible. Finally, the treated sections were counterstained with hematoxylin solution and after passing dehydration and clearing steps, they were mounted on glass slides. Selected sections from other groups were stained simultaneously as negative controls.

Quantification of positive immunoreacted cells

To investigate the probable survival and involvement of implanted hAdMSCs in the newly-formed bone tissue, the number of positive immuno-reacted cells for BrdU and osteocalcin were calculated separately under 100x magnification (19). The quantity of cells per unit area (N_A) was evaluated by using the succeeding formula in which $\sum Q$ is the sum total of counted osteocytes in the sections, *a/f* is the surface area correlated with each frame, and $\sum P$ is the totality of frame-related points hitting the described space (18).

$$\text{Newly-formed bone surface area} = \frac{\text{Measured bone surface area}}{[(\text{the whole area of the imaged graft surface}) - (\text{BCP granules surface area})]} \times 100$$

$$N_A = \frac{\sum \bar{Q}}{a/f. \sum P}$$

The obtained data were subjected to statistical analysis for any significant difference between the two values.

Statistical analysis

Statistical analysis was performed using SPSS 11.5 software package for windows. *In vitro* quantified data were analyzed statistically using repeated measures ANOVA, Kruskal-Wallis, and Mann-Whitney U tests; while *in vivo* data were analyzed using repeated measures ANOVA and Freidman tests. *P*-values lower than 0.05 were considered to be statistically significant.

Results

hAdMSC characterization and expansion

Isolated cells from adipose tissues were successfully cultured and passaged *in vitro*, with appearance characteristics of mesoderm-derived fibroblastic phenotype of MSCs. In addition, osteogenic and adipogenic differentiation of the cells were determined by the emergence of calcium deposits and lipid vacuoles, respectively (Figure 1). Expression of MSC markers was also confirmed by flow cytometry, as shown previously (12).

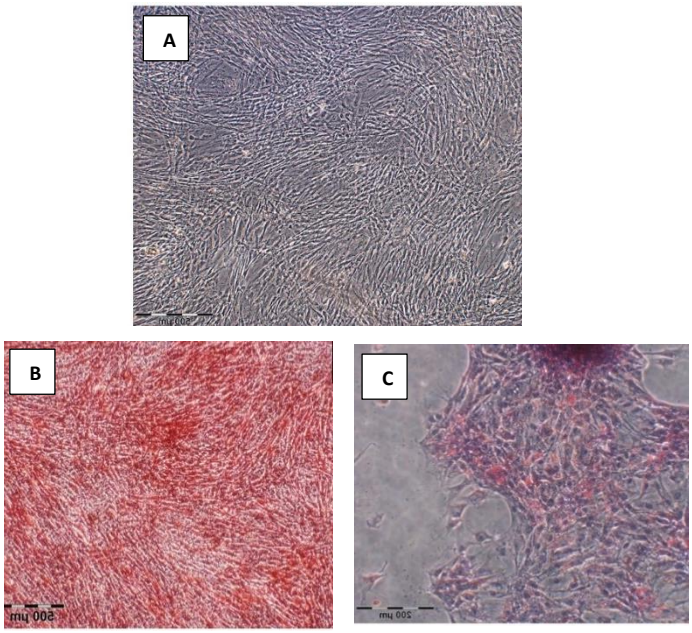

Figure 1. A. Undifferentiated human adipose-derived mesenchymal stem cells (hAdMSCs) representing characteristic mesoderm-derived fibroblastic phenotype; scale bar= 500 µm. B & C. characterization of hAdMSCs through *in vitro* differentiation of passage 3 (P3) cells towards osteogenic and adipogenic lineages. Panel (B) corresponds to osteogenesis confirmed by red-stained deposits of calcium via Alizarin Red (AZR) S staining; scale bar= 500 µm. Panel (C) corresponds to adipogenesis as confirmed by intracellular lipid vacuoles appeared in red via Oil red O staining; scale bar= 200 µm

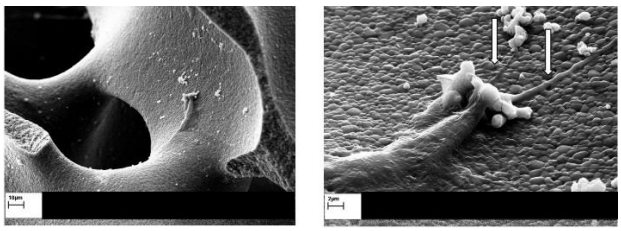

Figure 2. Scanning electron microscopy (SEM) observation of hydroxy-apatite/tricalcium-phosphate (HA/TCP) scaffolds cultured with human adipose-derived mesenchymal stem cells (hAdMSCs), representing fibroblastic cellular processes extended onto the scaffold after 24 hr of co-incubation (indicated by white arrows). Left: scale bar= 10 µm; right: scale bar= 2 µm

SEM evaluation

Qualitative SEM evaluation of hAdMSCs seeded on HA/TCP granules presented optimal cell adherence to the BCP ceramics as well as fibroblastic cellular processes extended onto the scaffold (Figure 2).

Cell proliferation assay

MTT assay revealed that application of HA/TCP scaffold (MT group) had a negative effect on the proliferation capacity of hAdMSCs. On the other hand, application of PRP and HA/TCP scaffold simultaneously (MTP group) significantly increased proliferation capacity of hAdMSCs in comparison to the MT group (P<0.01). However, the best results were obtained after treatment with PRP without HA/TCP (MP group), which led to a significantly higher proliferation capacity of hAdMSCs in comparison to MT (P<0.001) and MTP (P<0.01) groups. In each group, a decrease in the proliferation capacity of hAdMSCs was observed over time at 5 and 11 days after treatments. However, only the difference between day 3 and 11 was significant (P<0.05) (Figure 3).

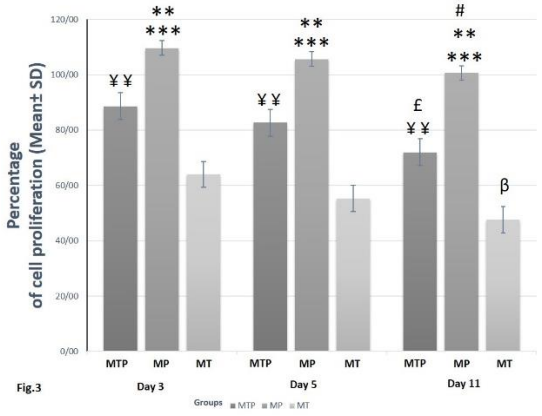

Figure 3. *In vitro* proliferation assessment of human adipose-derived mesenchymal stem cells (hAdMSCs) incubated with hydroxy-apatite/tricalcium-phosphate (HA/TCP) and/or platelet-rich plasma (PRP). Cell proliferation capacity of MP group was significantly increased when compared to MT (*** P<0.001) and MTP (** P<0.01) groups at each different day. Cell proliferation capacity of MTP group was significantly increased in comparison to MT group (¥¥P<0.01) at each different day. Cell proliferation capacity at day 11 was significantly decreased in MTP (£P<0.05), MP (#P<0.05) and MT (βP<0.05) groups as compared to the same group at day 3
MTP group= hAdMSCs + HA/TCP scaffold + PRP, MP group= hAdMSCs + PRP, MT= hAdMSCs + HA/TCP scaffold

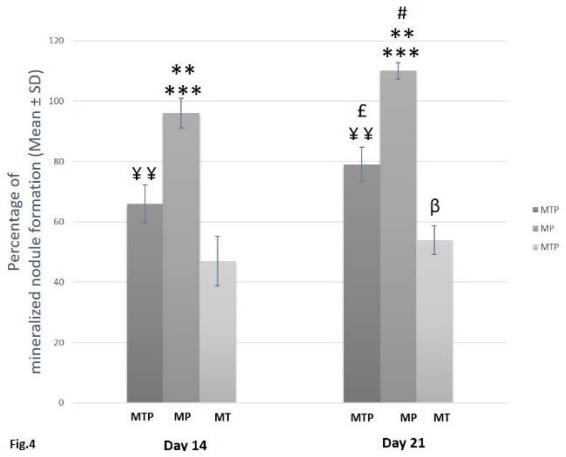

Figure 4: *In vitro* assessment for mineralized nodule formation of human adipose-derived mesenchymal stem cells (hAdMSCs) incubated with hydroxy-apatite/tricalcium-phosphate (HA/TCP) and/or platelet-rich plasma (PRP). Mineralized nodule formation capacity of MP group was statistically increased when compared to MT ($^{***}P$<0.001) and MTP ($^{**}P$<0.01) groups at each different day. Mineralized nodule formation capacity of MTP group was significantly increased in comparison to MT group ($^{¥¥}P$<0.01) at each different day. Mineralized nodule formation capacity of hAdMSCs was increased significantly at day 21 in MTP ($^{£}P$<0.05), MP ($^{\#}P$<0.05) and MT ($^{\beta}P$<0.05) groups as compared to the same group at day 14
MT= hAdMSCs + HA/TCP scaffold, MP group= hAdMSCs + PRP, MTP group= hAdMSCs + HA/TCP scaffold + PRP

Mineralized nodule formation

AZR S staining showed that co-incubation of hAdMSCs with 30 µg/ml pre-synthesized HA/TCP granules (MT group) in the osteogenic culture medium negatively affected mineralized nodule formation capacity of hAdMSCs. Supplementation of the osteogenic culture medium containing HA/TCP granules with PRP (MTP group) significantly enhanced mineralized nodule formation capacity of hAdMSCs in comparison to the MT group (P<0.01). However, PRP application alone (MP group) led to the significantly greatest amount of mineralized nodule formation of hAdMSCs in comparison to MT (P<0.001) and MTP (P<0.01) groups. In all groups, passing days from 14 to 21 led to a significant increase in the hAdMSCs capacity of mineralization (P<0.05) (Figure 4).

Figure 5. Macroscopic observation of wound healing at differently treated osseous defects of 4 experimental groups after 8 weeks (indicated by black arrows).
I= defective sites + autologous bone, II= defective sites left empty, III= defective sites + platelet-rich plasma (PRP) + hydroxy-apatite/tricalcium-phosphate (HA/TCP) scaffold, IV= defective sites + HA/TCP + PRP + human adipose-derived mesenchymal stem cells (hAdMSCs)

Macroscopic observation

The eight-week period of repair and recovery was uneventful in all the operated animals and no signs of hives, skin rash, or other unwanted immunologic reactions occurred to them at macroscopic observation. The defective sites of group I showed the best macroscopic healing after the 8-week period, with the borders of the defect almost disappearing and hard to recognize. However, empty defects of group II remained practically unrepaired, filled with a kind of soft granulation tissue to a relative extent. Other groups showed quite moderate healing (Figure 5).

Histological examination

AZR S-stained tissue sections from all of the five groups (n=5) were investigated by an optical microscope (Figure 6). No significant inflammatory cell infiltrate or foreign body reactions were found in the tissue sections of treated defects at microscopic examination. While the defective sites of group I were almost filled with mature bone trabeculae which looked nearly like the specimens from the normal control group, empty defects of group II were filled with soft tissue containing relatively sparse bone trabeculae. Tissue specimens of groups III and IV showed different amounts of woven bone trabeculae containing various-sized established marrow spaces.

Histomorphometrical analysis of newly-generated bone tissue

To investigate the impact of PRP and stem cell therapy on bone tissue regeneration, AZR S-stained sections of a total of 20 sample from 4 experimental groups were measured morphometrically for the percentage of mean (±SD) surface area of the newly-engineered bone tissue at defective osseous sites while this value was considered as 100% in the normal control group. The related values were (67.21%±5.77), (14.31%±3.46), (41.42%±2.08), and (54.53% ± 2.92) in groups I, II, III and IV, respectively (Figure 7).

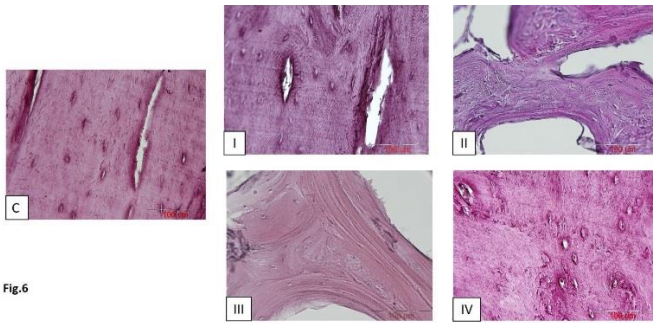

Figure 6. Alizarin Red S-stained sections of bone regeneration taken from 4 experimental groups as well as normal control specimens after 8 weeks; scale bar in all photos = 200 µm; C= normal control, I= defective sites + autologous bone, II= defective sites left empty, III= defective sites + platelet-rich plasma (PRP) + hydroxy-apatite/tricalcium-phosphate (HA/TCP) scaffold, IV= defective sites + HA/TCP + PRP + human adipose-derived mesenchymal stem cells (hAdMSCs)

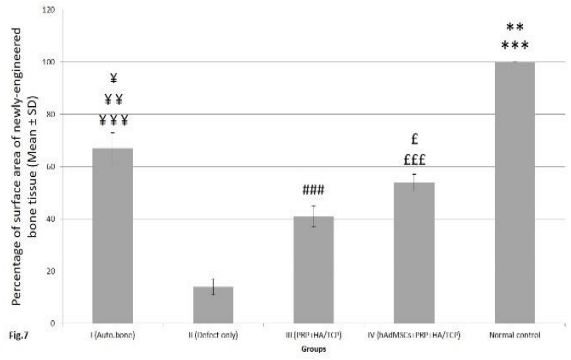

Figure 7. Quantitative evaluation of the percentage of mean (± SD) surface area of newly-engineered bone tissue at differently treated osseous defects of 4 experimental groups. This value was considered as 100% in the normal control group; control= normal control, I= defective sites +autologous bone, II= defective sites left empty, III= defective sites + platelet-rich plasma (PRP) + hydroxy-apatite/tricalcium-phosphate (HA/TCP) scaffold, IV= defective sites + HA/TCP + PRP + human adipose-derived mesenchymal stem cells (hAdMSCs). The percentage of the mean surface area of newly-engineered bone tissue in the normal control group was significantly higher when compared to that of groups I ($^{**}P$<0.01), II, III and IV ($^{***}P$<0.001). This value in group I was significantly higher comparing to those of groups II ($^{¥¥¥}P$<0.001), III ($^{¥¥}P$<0.01) and IV ($^{¥}P$<0.05). The percentage of the mean surface area of newly-engineered bone tissue in group IV was significantly higher than that of group II ($^{£££}P$< 0.001) and III ($^{£}P$<0.05). This value in group III was significantly higher than that of group II ($^{###}P$<0.001)

Our statistical analysis showed that the percentage of mean (± SD) surface area of newly-engineered bone tissue in the normal control group (considered as 100%) was significantly higher when compared to that of groups I (P<0.01), II, III and IV (P<0.001), respectively. In addition, the percentage of mean surface area of newly-engineered bone tissue in group I was significantly higher comparing to that of groups II (P<0.001), III (P<0.01) and IV (P<0.05), respectively. The percentage of mean surface area of newly-engineered bone tissue in group IV was significantly higher than that of group II (P<0.001) and III (P<0.05). In addition, this value in group III was significantly higher than that of group II (P<0.001) (Figure 7).

In vivo cell tracing

The immuno-histochemical reaction against osteocalcin protein of human origin showed its slight distribution throughout the bone matrix. In addition, the cytoplasm of a number of osteocytes positively reacted against this protein which was an indicator of their human origin (Figure 8). Furthermore, immune-histochemical verification of BrdU-labeled implanted stem cells into the defective sites of group IV (defective sites + HA/TCP scaffolds + PRP + hAdMSCs) revealed the presence of positive-reacted osteocytes throughout the newly-formed bone tissue. In our approach, existing BrdU-labeled cells appeared owing dark brown nuclei which were dispersed throughout purple nuclei belonging to the host animal (Figure 8).

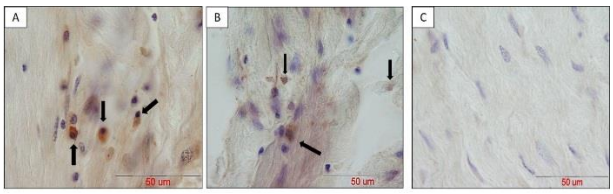

Figure 8. *In vivo* tracing of positive immune-reacted human adipose-derived mesenchymal stem cells (hAdMSCs) against human osteocalcin (panel A) and BrdU (panel B) in tissue sections of group IV (defective sites + platelet-rich plasma (PRP)+ hydroxy-apatite/tricalcium-phosphate (HA/TCP) scaffold + hAdMSCs) after 8 weeks (indicated by black arrows). Panel C indicates control slide to validate there is no specific binding of antibodies; scale bar in all photos = 50 µm

Quantification of positive immunoreacted cells

Quantity of positive immune-reacted cells against BrdU- labeled chromatin and osteocalcin-containing granules were measured as (1.67 ± 0.89) and (1.39 ± 0.78) per unit area (mm^2), respectively. Indeed, this value showed limited distribution in the bone tissue sections of group IV (defective sites +HA/TCP scaffolds + hAdMSCs +PRP). However, the two values presented no significant difference when compared to each other (Figure 9).

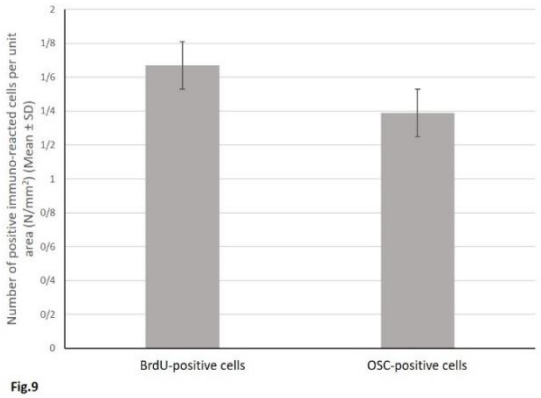

Figure 9. Quantitative assessment of the mean number (± SD) of positive immunoreacted cells per unit area (mm^2) of the new bone tissue; 1= BrdU-positive cells, 2= Osteocalcin -positive cells. The two values presented no significant difference when compared to each other

Discussion

This study aimed to evaluate the effect of pre-synthesized porous HA/TCP granules and PRP on the osteogenesis ability of hAdMSCs *in vitro* and *in vivo*. In addition, inserted hAdMSCs *in vivo* were traced to obtain more evidence on their biodistribution and possible contribution to bone tissue regeneration. *In vitro*, MTT assay revealed that 3, 5, and 11 days of co-incubation of hAdMSCs with 30 µg/ml HA/TCP granules significantly reduced the proliferation capacity of hAdMSCs, while passing days of co-incubation from day 3 to 11 inhibited the proliferation ability more significantly. However, PRP application in combination with HA/TCP granules augmented these capacities to a higher level. The best results were obtained when PRP was used alone at 3, 5, and 11 days of co-incubation with hAdMSCs. Indeed, PRP

treatment alone boosted the proliferation capacity of hAdMSCs in comparison to other groups. Furthermore, through AZR S staining, we found that 14 and 21 days of incubation of hAdMSCs with 30 µg/ml HA/TCP granules in the osteogenic culture medium significantly decreased mineralized nodule formation. Supplementing the osteogenic culture medium containing HA/TCP granules with PRP enhanced the mineralization capacity of hAdMSCs. However, PRP application alone led to acquiring the greatest outcomes of mineralized nodule formation after 14 and 21 days of incubation with hAdMSCs in the osteogenic culture medium. Unexpectedly, the results suggested that use of porous pre-synthesized HA/TCP granules significantly reduced the proliferation and mineralization capacity of hAdMSCs, while elimination of HA/TCP granules from the media supplemented with PRP considerably promoted these capacities. SEM evaluation of hAdMSCs sub-cultured with HA/TCP granules supported this finding, as cell distribution and attachment onto the HA/TCP granules was estimated moderately. Although some investigators have concluded that HA/TCP could be an appropriate scaffold for bone tissue engineering as it potentiated osteogenic differentiation of marrow cells *in vitro* and *in vivo,* it seems that further effects of HA/TCP granules on viability and osteogenic differentiation ability of hAdMSCs should be verified more precisely as this kind of biomaterial is very commonly used clinically (8). In this study, we decided to use a combination of HA/TCP granules and PRP *in vivo,* as a scaffold was needed for filling the surgically-created large osseous defects.

In vivo, treatment of osseous defects with the combination of HA/TCP granules and PRP led to significantly superior bone tissue healing response in comparison to non-treated defects. However, the capacity of osteoconductive HA/TCP granules consumed in this study to induce bone formation should be evaluated in more detail. Furthermore, stem cell application promoted bone tissue regeneration of osseous defects. However cell-based therapy could not attain the top ranking to become a comprehensive alternative for autologous bone grafting, which still remains the gold standard method in regenerative medicine (20, 21). Histomorphometrical analysis of the newly-formed bone surface area proved our claim. Moreover, the destiny of implanted stem cells that were mismatched to the host tissue, were traced via immunohistochemistry methods. Several recent studies have debated the disappearance of injected stem cells into the injury site and thus, proposed a paracrine constructive effect for MSCs, while other studies found few mismatched implanted stem cells of donor origin throughout the newly-formed bone tissue of host source (7, 22). In our study, we found that although the considerable part of new-engineered bone tissue was of host origin, osteocytes of human origin were incorporated into the fresh bone tissue and existed in the intimate neighborhood to the osteocytes of canine origin. However, morphometrical analysis revealed that only about 0.3% of the initial transplanted stem cells survived after an eight-week period *in vivo*. It has been hinted that MSC implantation into an osseous defect triggers a cascade of proangiogenic and host cell interesting events, which are central to the subsequent tissue repair and regeneration (23, 24).

PPR is an autologous natural composition of high concentrates of platelets, considered as a growth factor-delivery medium and employed as a proper alternative to a variety of administered growth factors in an attempt to stimulate the impressive healing response of host tissues (25). Upon degranulation, platelets become activated and release a wide range of pivotal mediators such as PDGF, VEGF, SDF-1, HGF, and IGF-1, which play a critical role in initiation of vasculogenesis and subsequent wound healing (3, 26). Beyond well-known bioactive components to neovasculogenesis contained in alpha granules of platelets, PRP has been assumed to include several numbers of cytokines introduced as stimulators of stem cell activation and mobilization (27). However, PRP application in regenerative procedures appears highly controversial; despite some findings regarding no significant relationship between use of PRP and enhancement of healing process, some investigators concluded the positive efficacy of PRP application in bone tissue regenerative procedures including sinus lifting methods, alveolar resorption after tooth extraction and even immediate implant loading techniques (28). Our findings were in line with the latter conclusions; since we found that PRP administration in combination with HA/TCP scaffold significantly improved the newly-formed bone area and thus, resulted in superior tissue regeneration than those in empty defects. Thus, the pivotal role of various growth factors contained in PRP in bone tissue regeneration has been implied.

Choosing a proper animal model in regenerative studies should be considered as an important issue. Bone structure of primitive rodents lacks Haversian systems and so, studying its repair may lead to obtaining misleading results far from those that would benefit human beings (29). In addition, inflammatory and regenerative procedures in large mammals are more similar to human beings than smaller ones (30). Dogs are the first choice of regulatory agencies like FDA in evaluation of the efficacy and safety of an applicable method to humans and thus, have been accepted as an appropriate animal model in orthopedic surgeries since a long time ago due to their similarities to human beings in the healing response of the bone tissue (31, 32).

However, limited number of defined groups and lack of some possible ones such as HA/TCP or PRP groups was one of the inadequacies of our study; but, reduction in the use of large animals persuaded us to perform the study with the mentioned defined groups.

According to previous studies, after creating a surgical defect, bone tissue reconstruction in canine species requires at least 6 weeks to become detectable in histological and morphometric analyses (33, 34). Therefore, we decided to perform our study on bone regeneration at 8 weeks post-surgery for more precise evidence. In addition, giving a longer period of time to animals might affect the percentage of newly-generated bone tissue, especially in MSC-received defects.

To the best of our knowledge, this is the first study conducted to investigate the *in vivo* fate and probable contribution of transplanted MSCs into canine large-sized osseous defects. This could be helpful in future speculation of stem cell therapy in clinical chair-side approaches.

Conclusion

We found that PRP application could enhance the proliferation and mineralization capacity of hAdMSCs incubated with HA/TCP granules *in vitro.* More-ever,

we found that cell-based therapy was able to promote bone tissue regeneration in alveolar bone defects of mongrel dog while only a few implanted MSCs of human origin were incorporated into the fresh bone tissue and existed in the intimate neighborhood to the host osteocytes of canine origin.

Acknowledgment

The authors thank the Vice-Chancellor for Research of Mashhad University of Medical Sciences, Mashhad, Iran for financial (support protocol code: 940024). The results presented in this paper were part of a PhD student thesis at Department of anatomy and cell biology. In addition, the authors gratefully appreciate the cooperation of Dr Nasser Sanjar- Moosavi in supplying liposuction material and also Dr. Hamed Abachizadeh for his expert technical assistance. Moreover, the authors thank the assistance of Fatemeh Motejaded and Abdollah Javan-Rashid.

Conflicts of interest

The authors declare no conflicts of interest.

Disclosure

The authors report no conflicts of interest concerning the materials or methods used in this study or the findings specified in this paper.

References

1. Mele L, Vitiello PP, Tirino V, Paino F, De Rosa A, Liccardo D, *et al.* Changing paradigms in cranio-facial regeneration: current and new strategies for the activation of endogenous stem cells. Front Physiol 2016; 7:62-69.
2. Chen W, Liu J, Manuchehrabadi N, Weir MD, Zhu Z, Xu HH. Umbilical cord and bone marrow mesenchymal stem cell seeding on macroporous calcium phosphate for bone regeneration in rat cranial defects. Biomaterials 2013; 34:9917-9925.
3. Xie X, Wang Y, Zhao C, Guo S, Liu S, Jia W, *et al.* Comparative evaluation of MSCs from bone marrow and adipose tissue seeded in PRP-derived scaffold for cartilage regeneration. Biomaterials 2012; 33:7008-7018.
4. Haddad-Mashadrizeh A, Bahrami AR, Matin MM, Edalatmanesh MA, Zomorodipour A, Fallah A, *et al.* Evidence for crossing the blood barrier of adult rat brain by human adipose-derived mesenchymal stromal cells during a 6-month period of post-transplantation. Cytotherapy 2013; 15:951-960.
5. Li Q, Wang T, Zhang Gf, Yu X, Zhang J, Zhou G, *et al*. A comparative evaluation of the mechanical properties of two calcium phosphate/collagen composite materials and their osteogenic effects on adipose-derived stem cells. Stem Cell Int 2016; 2016:6409546.
6. Azevedo A, Sá M, Fook M, Neto PN, Sousa O, Azevedo S, *et al.* Use of chitosan and β-tricalcium phosphate, alone and in combination, for bone healing in rabbits. J Mater Sci Mater Med 2014; 25:481-486.
7. Gamblin A-L, Brennan MA, Renaud A, Yagita H, Lézot F, Heymann D, *et al.* Bone tissue formation with human mesenchymal stem cells and biphasic calcium phosphate ceramics: the local implication of osteoclasts and macrophages. Biomaterials 2014; 35:9660-9667.
8. Sulaiman SB, Keong TK, Cheng CH, Saim AB, Idrus RB. Tricalcium phosphate/hydroxyapatite (TCP-HA) bone scaffold as potential candidate for the formation of tissue engineered bone. Indian J Med Res 2013; 137:1093-1098.
9. Tollemar V, Collier ZJ, Mohammed MK, Lee MJ, Ameer GA, Reid RR. Stem cells, growth factors and scaffolds in craniofacial regenerative medicine. Gen Dis 2016; 3:56-71.
10. Burnouf T, Strunk D, Koh MB, Schallmoser K. Human platelet lysate: Replacing fetal bovine serum as a gold standard for human cell propagation? Biomaterials 2016; 76:371-387.
11. Anitua E, Prado R, Padilla S, Orive G. Platelet-rich plasma therapy: another appealing technology for regenerative medicine? Reg Med 2016; 11:355-357.
12. Bidkhori HR, Ahmadiankia N, Moghaddam Matin M, Farshchian M, Naderi-meshkin H, Shahriyari M, *et al.* Chemically primed bone-marrow derived mesenchymal stem cells show enhanced expression of chemokine receptors contributed to their migration capability. Iran J Basic Med Sci 2016; 19:14-19.
13. LeGeros RZ. Properties of osteoconductive biomaterials: calcium phosphates. Clin Orthop Relat Res 2002; 395:81-98.
14. Nagyova M, Slovinska L, Blasko J, Grulova I, Kuricova M, Cigankova V, *et al*. A comparative study of PKH67, DiI, and BrdU labeling techniques for tracing rat mesenchymal stem cells. In Vitro Cell Dev Biol Anim 2014; 50:656-663.
15. Kang Y, Kim S, Khademhosseini A, Yang Y. Creation of bony microenvironment with CaP and cell-derived ECM to enhance human bone-marrow MSC behavior and delivery of BMP-2. Biomaterials 2011; 32:6119-6130.
16. Tavakolinejad S, Khosravi M, Mashkani B, Bideskan AE, Mossavi NS, Parizadeh MR, *et al.* The effect of human platelet-rich plasma on adipose-derived stem cell proliferation and osteogenic differentiation. Iran Biomed J 2014; 18:151-159.
17. Rentsch C, Schneiders W, Manthey S, Rentsch B, Rammelt S. Comprehensive histological evaluation of bone implants. Biomatter 2014; 4:27993.
18. Mohammadipour A, Fazel A, Haghir H, Motejaded F, Rafatpanah H, Zabihi H, *et al.* Maternal exposure to titanium dioxide nanoparticles during pregnancy; impaired memory and decreased hippocampal cell proliferation in rat offspring. Environ Toxicol Pharmacol 2014; 37:617-625.
19. Stern MH, Mackler BF, Dreizen S. A quantitative method for the analysis of human periapical inflammation. J Endod 1981; 7:70-74.
20. Raposo-Amaral CE, Bueno DF, Almeida AB, Jorgetti V, Costa CC, Gouveia CH, *et al.* Is bone transplantation the gold standard for repair of alveolar bone defects? J Tissue Eng 2014; 5:2041731413519352.
21. Griffin M, Kalaskar DM, Butler PE, Seifalian AM. The use of adipose stem cells in cranial facial surgery. Stem Cell Rev Rep 2014; 10:671-685.
22. Brennan MÁ, Renaud A, Amiaud J, Rojewski MT, Schrezenmeier H, Heymann D, *et al.* Pre-clinical studies of bone regeneration with human bone marrow stromal cells and biphasic calcium phosphate. Stem Cell Res Ther 2014; 5:1-15.
23. Seebach E, Freischmidt H, Holschbach J, Fellenberg J, Richter W. Mesenchymal stroma cells trigger early attraction of M1 macrophages and endothelial cells into fibrin hydrogels, stimulating long bone healing without long-term engraftment. Acta Biomater 2014; 10:4730-4741.

24. Mathieu M, Rigutto S, Ingels A, Spruyt D, Stricwant N, Kharroubi I, *et al*. Decreased pool of mesenchymal stem cells is associated with altered chemokines serum levels in atrophic nonunion fractures. Bone 2013; 53:391-398.
25. Chen FM, Zhang M, Wu ZF. Toward delivery of multiple growth factors in tissue engineering. Biomaterials 2010; 31:6279-6308.
26. Martínez CE, Smith PC, Palma Alvarado VA. The influence of platelet-derived products on angiogenesis and tissue repair: a concise update. Front Physiol 2015; 6:290.
27. Fekete N, Gadelorge M, Fürst D, Maurer C, Dausend J, Fleury-Cappellesso S, *et al.* Platelet lysate from whole blood-derived pooled platelet concentrates and apheresis-derived platelet concentrates for the isolation and expansion of human bone marrow mesenchymal stromal cells: production process, content and identification of active components. Cytotherapy 2012; 14:540-554.
28. Albanese A, Licata ME, Polizzi B, Campisi G. Platelet-rich plasma (PRP) in dental and oral surgery: from the wound healing to bone regeneration. Immun Ageing 2013; 10:1-10.
29. Nunamaker D. Experimental models of fracture repair. Clin Orthop Relat Res 1998; 355:56-65.
30. Kovacevic M, Tamarut T, Zoricic S, Bešlic S. A method for histological, enzyme histochemical and immunohisto-chemical analysis of periapical diseases on undecalcified bone with teeth. Acta Stomatol Croat 2003;37:261-273.
31. Pearce S. Animal models for bone repair. Eur Cell Mater 2007; 14:42-49.
32. Pearce A, Richards R, Milz S, Schneider E, Pearce S. Animal models for implant biomaterial research in bone: a review. Eur Cell Mater 2007;13:1-10.
33. Ito K, Yamada Y, Nakamura S, Ueda M. Osteogenic potential of effective bone engineering using dental pulp stem cells, bone marrow stem cells, and periosteal cells for osseointegration of dental implants. Int J Oral Maxillofal Implants 2011; 26:947-954.
34. Jafarian M, Eslaminejad MB, Khojasteh A, Abbas FM, Dehghan MM, Hassanizadeh R, *et al.* Marrow-derived mesenchymal stem cells-directed bone regeneration in the dog mandible: a comparison between biphasic calcium phosphate and natural bone mineral. Oral Surg Oral Med Oral Pathol Oral Radiol Endod 2008; 105:14-24.